Biomass Conversion and Biorefinery (2024) 14:11011–11022
https://doi.org/10.1007/s13399-022-03136-2

ORIGINAL ARTICLE

Green synthesis of sulfonated graphene oxide-like catalyst from corncob for conversion of hemicellulose into furfural

Ninh Thi Tinh[1,2,3] · Nguyen Thi Phuong[1,2,3,4] · Do Gia Nghiem[1,2,3] · Do Khanh Dan[1,2,3] · Pham Tan Khang[1,2,3] · Nguyen Minh Dat[1,2,3] · Huynh Thi Tuong Vy[1,2,3] · Le Minh Huong[1,2,3] · Tat Minh Hoang[1,2,3] · Mai Thanh Phong[1,2,3] · Nguyen Huu Hieu[1,2,3]

Received: 16 May 2022 / Revised: 18 July 2022 / Accepted: 20 July 2022 / Published online: 28 July 2022

Abstract

The development of an environmentally friendly synthesized biomass-derived catalyst for the conversion of hemicellulose to platform chemicals has attracted worthwhile attention. In this work, an acidic carbon-based catalyst (C-SGO) with a structure resembling sulfonated graphene oxide is synthesized from corncob-extracted cellulose by bleaching, alkalization, carbonization, and sulfonation processes. Characteristics of the as-synthesized C-SGO were investigated using Fourier-transform infrared spectroscopy, X-ray diffraction spectroscopy (XRD), Raman spectroscopy, energy dispersive spectroscopy, thermal gravimetric analysis, Brunauer–Emmett–Teller, and scanning electron microscopy (SEM). Raman spectrum of C-SGO spectroscopy indicated the existence of D and G bands at 1338.72 and 1593.41 cm^{-1}, respectively. SEM images of C-SGO showed sheet-like structures with folds and wrinklier after the sulfonation process, confirming the structural similarity of the synthesized material to sulfonated graphene oxide sheets. The synthesized C-SGO catalysts were applied for the conversion of hemicellulose from corncob to furfural. The synergistic effect of C-SGO and the concentration of NaCl 0.2 mol/L in the furfural synthesis reaction achieved a yield of 40.03% at a temperature of 200 °C, time of 90 min, and 100 mg of the catalyst amount, showing the potential of using seawater or wastewater containing NaCl as a low-cost solvent. Moreover, the catalyst also demonstrated reusability after 5 cycles, showing that C-SGO can be used as a heterogeneous catalyst suitable for furfural synthesis.

Keywords Sulfonated graphene oxide-like carbon acid · Furfural · Corncob

1 Introduction

Hemicellulose is the one of main compounds in lignocellulosic biomass, a promising biofuel precursor as a replacement for fossil fuels. During chemical processes, hemicellulose is first hydrolyzed to pentose sugars (xylose, arabinose) in the liquid phase and then further dehydrated into furfural as the main product [1]. Furfural is one of the promising platform chemicals widely used in petroleum refining, plastics, pharmaceutical, and chemical industries [2]. In the manufacturing industry, furfural is synthesized directly from biomass by homogeneous acid catalysts such as H_2SO_4 and H_3PO_4 because of their good dispersion ability, simple synthesis, and low cost [3]. However, the difficulty of recovering the solvent after the reaction results in difficulties in catalyst separation and recovery, equipment corrosion, and overall environmental damage [4]. An increasing number of researchers are consequently focused on heterogeneous catalytic syntheses, utilizing materials

✉ Nguyen Huu Hieu
nhhieubk@hcmut.edu.vn

1 VNU-HCM Key Laboratory of Chemical Engineering and Petroleum Processing (Key CEPP Lab), Ho Chi Minh City University of Technology (HCMUT), 268 Ly Thuong Kiet Street, District 10, Ho Chi Minh City, Vietnam

2 Faculty of Chemical Engineering, Ho Chi Minh City University of Technology (HCMUT), 268 Ly Thuong Kiet Street, District 10, Ho Chi Minh City, Vietnam

3 Vietnam National University Ho Chi Minh City (VNU-HCM), Linh Trung Ward, Thu Duc City, Ho Chi Minh City, Vietnam

4 Ho Chi Minh City University of Food Industry (HUFI), 140 Le Trong Tan Tay Thanh Ward Tan Phu District, Ho Chi Minh City, Vietnam

such as zeolites, polymers, metal oxides, and carbon-based catalysts because of their superior properties and ease of recovery after operation [5].

Carbon-based materials have attracted worthwhile attention in research with special properties such as high mechanical strength, hydrothermal stability, large surface area, and tunable surface functional groups [6]. In general, carbon-based catalysts have been greatly successful in converting biomass material into furfural. Various synthesis strategies have been employed to modify carbon-based materials with a diversity of functional groups: a resorcinol–formaldehyde resin carbon catalyst synthesized with sulfanilic acid as the sulfonating agent achieved a xylose-to-furfural conversion efficiency of nearly 100% and overall furfural yield reaching 80% [7]. Alternatively, a carbonized sulfonated teff straw-based material (CST) provided a conversion efficiency from xylose into furfural of 62.4% [8], and a sulfonated graphene material synthesized from graphite has a furfural yield from xylose of 96% and a SO_3H-NG-C material sourced from glucosamine managed to convert corn stalk into furfural with 53% overall efficiency [6]. Among carbon-based structures are graphene-based materials, specifically graphene oxide (GO) which possesses noteworthy thermal, electrical, chemical, optical, and catalytic properties [9, 10]. GO can be synthesized through the oxidation and delamination of graphite. The oxidation process allows oxygen-containing functional groups to attach to the surface of the material, such as epoxy groups on the carbon lattice plane and small amounts of carbonyl and carboxyl groups at the plate edges [11, 12]. Additionally, GO is considered a potential acid catalyst for conversion reactions due to its good dispersion in water. Several methods of GO synthesis are known, such as chemical vapor deposition (CVD) and mechanical ablation. However, the above methods require complex synthesis, high cost, and generate many harmful emissions such as NO_2, N_2O_4, and ClO_2 [13]. Recently, there are more and more studies on synthesizing materials structurally similar to GO from biomass because of its easy access, rapid regeneration, low cost, and environmental friendliness [14]. Examples of recent research include synthesizing GO and graphene quantum dots using *Miscanthus* as a precursor via an ultrasound-assisted mechano-chemical cracking method [15], synthesizing sulfonated graphene from nettle leaves [14] and GO from coconut shell waste [11]. Besides, to improve furfural yield, the addition of sulfonic groups ($-SO_3H$) to increase the acidity of the material plays an important role in converting hemicellulose to furfural [16, 17]. The $-SO_3H$ group is assigned as the Brønsted acid site along with other acidic functional groups such as − COOH and C − OH, which participate in hydrolysis; H^+ and water react together to cleave the C − O bond in β-1,4-glycosidic and then dehydrate to form furfural [18].

In this study, cellulose-derived sulfonated graphene oxide-like catalyst (C-SGO) was synthesized from corncob by bleaching, alkalization, carbonization, and sulfonation processes. The effects of calcination time, cellulose:ferrocene ratio on the characteristics of cellulose-derived graphene oxide-like (C-GO), and C-SGO catalysts were studied through Fourier-transform infrared spectroscopy (FTIR), X-ray diffraction spectroscopy (XRD), Raman spectroscopy, energy dispersive spectroscopy (EDS), thermal gravimetric analysis (TGA), Brunauer–Emmett–Teller (BET), and scanning electron microscopy (SEM). The catalytic ability of the materials in terms of the furfural yield was also investigated with constant parameters at 200 °C in 90 min and 10 wt% amount of catalyst. The synthesis of C-SGO from biomass opens up a potential direction of application that helps to solve the issue of biomass residues. The reusability of C-SGO material after five cycles was also investigated.

2 Materials and methods

2.1 Materials and chemicals

Corncob was collected from Dong Nai province, Vietnam. Furfural ($C_5H_4O_2$, 99%) was purchased from Fisher Scientific Co. Ltd. 3,5-Dinitrosalicylic acid ($C_7H_4N_2O_7$, 98%) and xylose ($C_5H_{10}O_5$) were purchased from Sigma Aldrich Co. Ltd, USA. Sulfuric acid (H_2SO_4, 98%), sodium hydroxide (NaOH, 99.8%), ferrocene ($C_{10}H_{10}Fe$), hydrochloric acid (HCl, 36.5%), sodium chlorate ($NaClO_2$), methanol (CH_3OH, 99.5%), and ethanol (C_2H_5OH, 95%) were purchased from Xilong Scientific Co. Ltd, China. All chemicals were used without any further purification. Double-distilled water was used in all experiments.

2.2 Pretreatment of corncob

2.2.1 Extraction of hemicellulose

Corncob was washed, dried at 60 °C for 24 h, and then ground into small pieces. Five g of corncob was added to 75 mL of 2 M NaOH, and the mixture was heated to 90 °C with continuous stirring for 2 h. The corncob was filtered out and washed with 2 mL 0.1 N NaOH. The filtrated solution was adjusted to pH 5 with HCl, and 95% ethanol was added to the mixture until precipitate appeared. Hemicellulose was obtained by filtering the precipitate and drying at 80 °C for 24 h, while the remaining cellulose residue was dried [19].

Determination of D-xylose in hemicellulose was carried out by the dinitrosalicylic acid (DNS) method on a UV–Vis spectrophotometer (Dual-FL, Horiba) at a wavelength of 530 nm [20].

2.2.2 Extraction of cellulose

The cellulose residue obtained was subsequently delignified. Firstly, 0.635 wt% $NaClO_2$ was added, and the mixture was stirred at 60 °C for 6 h. The obtained cellulose powder was washed with distilled water to neutral pH and dried to constant weight before being used to synthesize C-GO.

The separation efficiency of hemicellulose and cellulose (%) from corncob was calculated as given by Eqs. (1) and (2):

$$\text{Cellulose yield (\%)} = \frac{\text{mass of cellulose (g)}}{\text{mass of corncob}} \times 100 \quad (1)$$

$$\text{Hemicellulose yield (\%)} = \frac{\text{mass of hemicellulose (g)}}{\text{mass of corncob}} \times 100 \quad (2)$$

2.3 Preparation of catalysts

2.3.1 Synthesis of C-GO from the cellulose of corncob

Cellulose powder was mixed with ferrocene in a crucible, and the mixture was reacted in a furnace [13]. The black solid obtained was labeled as C-GO. Samples synthesized at different calcination times with different precursor ratios are denoted as summarized in Table 1. In addition, GO synthesized from graphite via the improved Hummers method was used as a control [12].

2.3.2 Synthesis of C-SGO

C-SGO was synthesized using sulfuric acid as a reagent [21]. One g of C-GO was added to a mixture of 20 mL methanol and 15 mL of H_2SO_4 1 M and then sonicated for 1 h to create a homogeneous suspension. The mixture was dried at 100 °C for 24 h, filtered, and washed with ethanol until neutral pH was achieved. Subsequently, the solution was dried at 80 °C for 6 h to acquire C-SGO.

Table 1 Effect of different conditions on C-GO synthesis investigation

No	Samples	Calcination time (min)	Cellulose:ferrocene ratio (wt:wt)
1	C-GO1	15	1:1
2	C-GO2	30	
3	C-GO3	60	
4	C-GO4	90	
5	C-GO5	120	
6	C-GO6	30	1:5
7	C-GO7		1:3
8	C-GO8		1:1
9	C-GO9		3:1
10	C-GO10		5:1

2.4 Characterization of materials

FTIR was used to identify functional groups in the material (Alpha-E, Bruker Optik GmbH, Ettlingen, Germany), with potassium bromide (KBr) pellets in the wavenumber range between 400 and 4000 cm^{-1}. The morphological structure was investigated via XRD measured on an Advanced X8, Bruker ($\lambda_X = 0.154$ nm), with CuK_α irradiation in the range of 5–80° (D2 Phaser, Bruker, Germany). The elemental composition of materials was determined using EDS (Jeol–JMS 6490, Japan). SEM images (S–4800, Hitachi, Japan) were obtained at an accelerating voltage of 100 kV to study the surface structure of C-GO and C-SGO materials, accordingly. The recording of N_2 adsorption/desorption isotherms of catalyst was carried out prior to the degassing at 77 K and recorded on an Autosorb iQ gas sorption analyzer (Quantachrome Instruments, USA). The specific surface area of the catalyst was determined using Brunauer–Emmett–Teller method, and the pore was detected by the density functional theory (DFT) method. Thermogravimetry analysis was from 20 to 800 °C at a rate of 10 °C min^{-1} in the air on a Setaram TGA.

2.5 Conversion of hemicellulose to furfural

2.5.1 Effect of material synthesis conditions on furfural yield

Furfural was synthesized from hemicellulose via hydrolysis and dehydration. First, the C-SGO suspension was added to the hemicellulose mixture. The mixture was placed in the Parr 4848 high-pressure reactor and reacted at a temperature of 200 °C, with a reaction time of 90 min and a catalyst amount of 100 mg. After condensing the resulting vapor and cooling to room temperature, the post-reaction mixture was filtered, and the filtrate was analyzed via UV–Vis spectrophotometry (Dual-FL, Horiba) at the wavelength of 278 nm [19].

In order to determine the suitable synthesis conditions for C-SGO, the various synthesized samples were evaluated with respect to their catalytic ability. The furfural yield (%) from hemicellulose was calculated as given by Eq. (3) [22]:

$$\text{Furfural yield(\%)} = \frac{\text{moles of furfural in the product (mol)}}{\text{moles of initial xylose (mol)}} \times 100 \quad (3)$$

2.5.2 Effect of NaCl concentration on furfural yield

Effects of NaCl concentration (0–0.5 mol/L) on furfural yield were investigated at 200 °C for 90 min with the initial catalyst dosage of 100 mg. The possible reaction conversion route of hemicellulose to furfural with the presence of the acid catalyst and NaCl was simplified, as shown in Scheme 1.

2.5.3 Reusability of the C-SGO catalyst

To investigate the reusability of C-SGO, the reaction was carried out at 200 °C for 90 min with 100 mg catalyst. After each batch of reactions, the catalyst was recovered by filtration, washed with ethanol and distilled water several times, and dried at 80 °C in the oven overnight.

3 Results and discussion

3.1 Pretreatment of corncob

The pretreatment process of corncob plays a vital role in the synthesis process of furfural. Through alkalization, the obtained hemicellulose was used as the substrate for the synthesis process of furfural. Besides, the cellulose was delignified and used for catalyst synthesis, making maximal use of the biomass. Table 2 shows the separation efficiency of hemicellulose and cellulose from corncob in this study in comparison with other methods. According to the results, the efficiency of detaching hemicellulose impacted by alkalizing agent NaOH 2 M was 60.43%. This can be explained by the selective alkalization of hemicellulose, which breaks down the cell wall through hydrolysis of the ester bond between hemicellulose and lignin [23]. Additionally, the ionization of phenolic groups of lignin and carboxyl groups

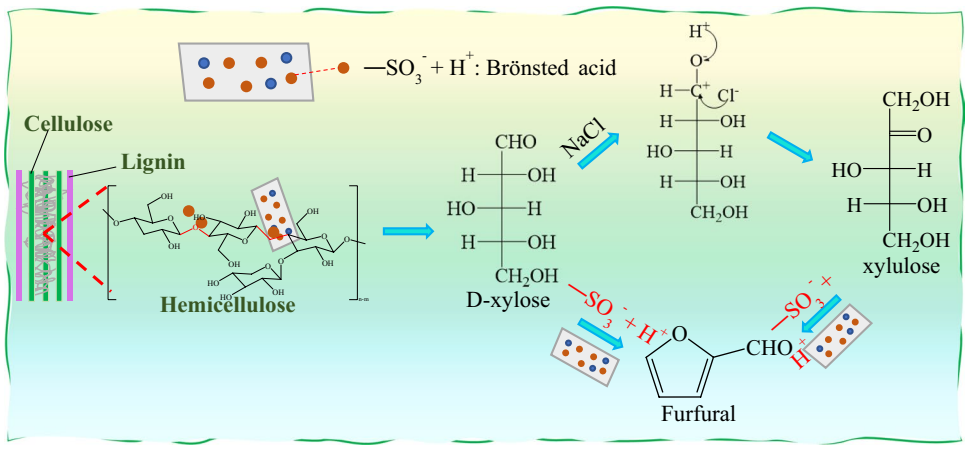

Scheme 1 Possible reaction conversion route of hemicellulose to furfural

Table 2 Separation efficiency of hemicellulose and cellulose from corncob

No	Method	Chemical compounds	Separation efficiency (%)	Ref
1	0.635 wt% NaOH 2 M	Cellulose	27.56	This study
2		Hemicellulose	60.43	This study
3	Distilled water, 80 °C, 24 h	Hemicellulose	6.25	[25]
4	2% NaOH, 90 °C, 2 h	Hemicellulose	67.44	
5	EtOH:NaOH (20:1), 60 °C, 3 h	Hemicellulose	3.95	
6	Soaking in aqueous ammonia	Cellulose	45.7	[26]
		Hemicellulose	> 50	
7	Liquid hot water	Cellulose	84.73	[27]
		Hemicellulose	4.58	
		Lignin	10.68	
8	Hydrothermal	Cellulose	78.34	[28]
		Hemicellulose	7.95	
		Lignin	17.7	

of hemicellulose may enhance the dissolving ability of the hemicellulose while simultaneously decreasing the crystallinity of cellulose fibers via swelling in the alkaline environment. This ultimately accelerates the release of residual hemicellulose and lignin. Besides that, the dissolution of hemicellulose is proportional to the alkali concentration — which implies greater biomass separation capability [24]. It is notable that the method utilizing liquid hot water returned the greatest proportion of cellulose (84.73%) while conversely yielding the least hemicellulose (4.58%). However, considering the objective of producing furfural from hemicellulose, the method using NaOH 2 M is deemed appropriate for this research.

As shown in Fig. 1, FTIR spectra show the difference in bonding present in the components of the biomass. A peak at the wavelength of 3300–3400 cm^{-1} is observed in all three samples, representing the stretching fluctuation of the − OH group. An additional signal at 2921.76 cm^{-1} characterizes the vibration of C_{sp3} − H, which is indicative of the carbon network in the material [29]. The appearance of acetyl groups in xylan is confirmed via the absorption band at 1562.13 cm^{-1}, which correlates to C = O aldehyde bonds in an amorphous state. The absorption band at 1562.13 cm^{-1}, on the other hand, may be attributed to the aromatic C = C ring stretching and C − H deformation in methyl, methylene, and methoxyl groups from lignin impurities [30]. Such peaks, however, completely disappear in the spectrum of cellulose, which confirms the successful delignification process of cellulose after separation. Furthermore, a small peak at 895.85 cm^{-1} affirms the presence of β-1,4-glycosidic bonding. Absorption bands at 1416.15 and 1348.17 cm^{-1} are identified as C − H bending in hemicellulose, the existence

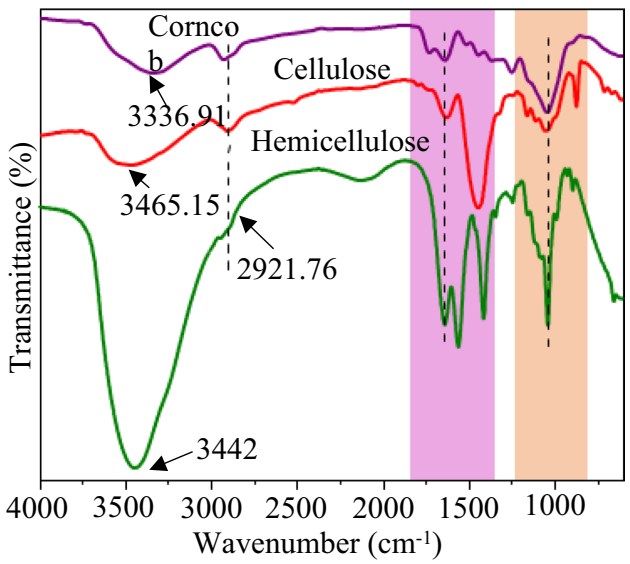

Fig. 1 FTIR spectra of corncob, cellulose, and hemicellulose

of which is further confirmed by the absorption band at 1044.21 cm^{-1} characteristics of C − O, C − C, and C − OH vibrations [31].

The SEM of corncob, as shown in Fig. 2a, illustrates a rough surface with many microparticles, fibers, and small blocks characteristic of lignin without corrugated sheets and the cell structure without obvious porous structure. Corncob is comprised of different components including the beeswing, woody ring, and pith — each of which has a different form and structure with varying cellulose, hemicellulose, lignin, and wax content [28]. Treatment with NaOH can separate the block form and inter-fiber lignin, leading to the breakage and dispersion of biomass fibers. After removing the lignin and obtaining cellulose as shown in Fig. 2b, naked microfibril bundles are identified with uneven distribution and a compacted sheet structure. Figure 2c illustrates the morphology of the hemicellulose obtained from alkalization; an amorphous mesoporous structure can be observed. Hemicellulose particles did not evenly distribute rough surface with cracks. Hemicellulose obtained from corncobs is obtained from amorphous insoluble macromolecular compounds, which have a more compact structure than the polyporous structure from other biomass sources such as rapeseed and straw. This can be explained, depending on the type of biomass that the obtained components also have different morphology, respectively [32, 33].

3.2 Effect of C-GO material synthesis conditions on furfural yield

The FTIR spectra of GO and C-GO materials at different calcination times, such as 15, 30, 60, 90, and 120 min assigned to C-GO1, C-GO2, C-GO3, C-GO4, and C-GO5, respectively, are shown in Fig. 3a. The results show a broad peak around 3400–3600 cm^{-1} attributed to the stretching vibrations of hydroxyl groups of interlayer water molecules. In comparison to GO from commercial graphite, the FTIR spectra of C-GO materials from cellulose exhibit the presence of various oxygen functional groups in ranges of 1700–1710 cm^{-1} (C = O stretching vibrations) and 1610–1620 cm^{-1} (COOH stretching vibrations) which show the characteristic peak of GO. In particular, the C-GO2 material calcined at 30 min shows similar peaks to those in the FTIR spectrum of GO at 1380.93 and 1045 cm^{-1} assigned to the stretching vibration of the C − OH and C − O bonding [10]. It becomes a desirable candidate with respect to its similarity to GO. However, to select catalyst materials for high furfural yield, materials that were investigated for catalytic efficiency of furfural synthesis are shown in Table 3. The result shows that, for C-GO2 material, the furfural yield is highest, at 27.79 ± 0.51%, compared to the different times of the same calcination temperature. Thus, C-GO2 is chosen to investigate the ratio of cellulose:ferrocene.

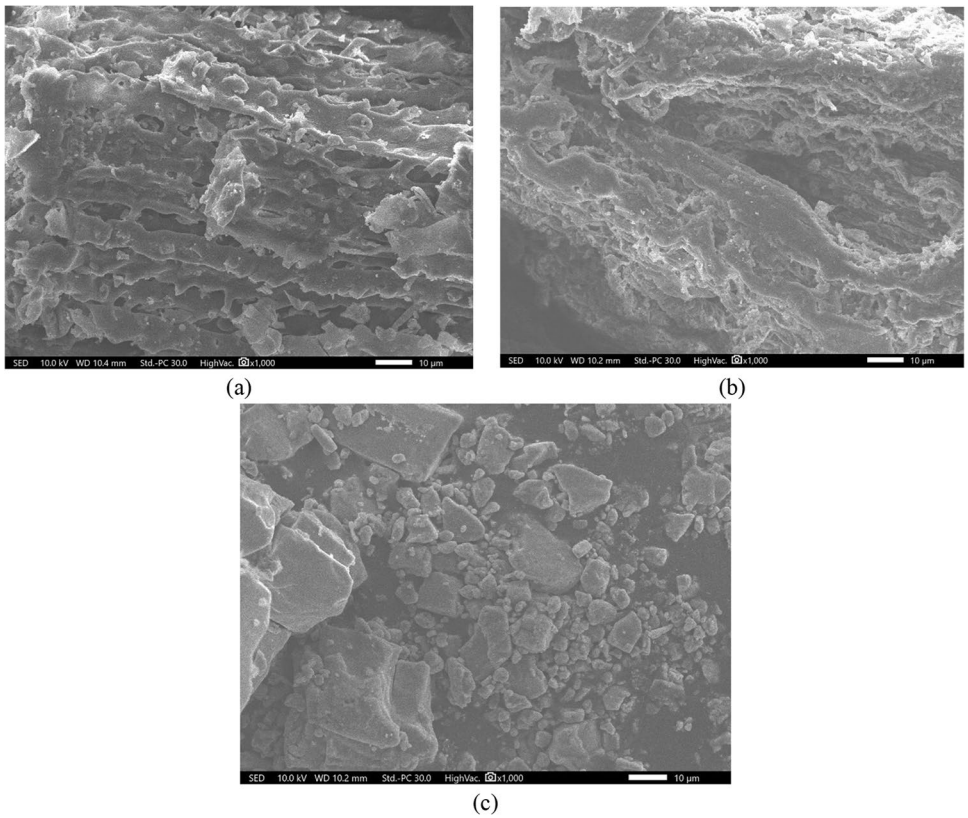

Fig. 2 SEM images of **a** raw corncob, **b** cellulose, and **c** hemicellulose of corncob

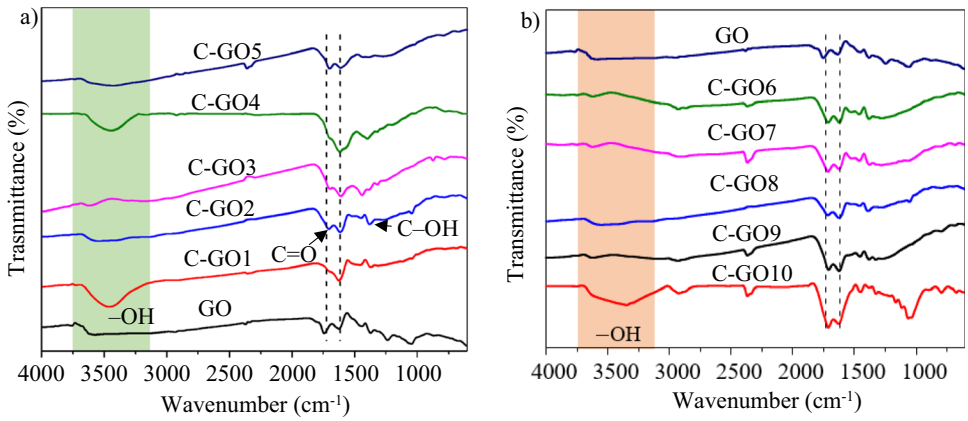

Fig. 3 FTIR spectra of C-GO at **a** different calcination times and **b** cellulose:ferrocene ratios

Table 3 Effect of C-GO material synthesis conditions on furfural yield

Samples	Furfural yield (%)	Samples	Furfural yield (%)
C-GO1	12.67 ± 0.53	C-GO6	21.72 ± 0.32
C-GO2	27.79 ± 0.51	C-GO7	23.58 ± 0.34
C-GO3	25.54 ± 0.23	C-GO8	27.79 ± 0.51
C-GO4	22.42 ± 0.34	C-GO9	23.25 ± 0.20
C-GO5	15.86 ± 0.23	C-GO10	19.73 ± 0.39

Figure 3b displays the FTIR spectra of C-GO samples calcinated with different ratios of cellulose:ferrocene. Compared to the remaining materials, the C-GO5 sample calcined with the cellulose:ferrocene ratio of 5:1 demonstrated a stark difference in intensity at the wavelength range of 3300–3600 cm^{-1} assigned to the extension of the − OH bond (hydroxyl group). In addition, the presence of peaks at 2917.82 cm^{-1} was attributed to C − H stretching, due to the presence of C − H groups of cellulose. Besides, the

C-GO10 sample has the presence of strong intensity peaks at 1053.84 and 1157.99 cm^{-1} which are attributed to the pyranose ring stretching vibration in the asymmetric C − O − C phase [34]. Therefore, the C-GO10 material still retains the characteristic peaks in the structure of cellulose. For samples C-GO6 and C-GO7, the peaks at 2924.18, 2924.38, and 2855.29 cm^{-1} are attributed to the fatty C–H fluctuations due to ethanolamine and ferrocenyl alkyl radicals [35]. This could be explained by the much higher ratio of catalysts compared to cellulose. Except for the GO sample from graphite and C-GO8, the remaining samples possess sharp absorption peaks at positions 2359.21, 2365.44, 2366.22, and 2360.76 cm^{-1} for C-GO6, C-GO7, C-GO9, and C-GO10, respectively, assigned to C − O bonding [36]. In addition, the effect of cellulose:ferrocene ratio on furfural yield is also investigated. Notably, C-GO8 material shows the highest furfural yield, at 27.79 ± 0.51%, compared to other materials, and FTIR spectra show characteristic peaks most similar to GO. As a result, C-GO8 material is used to synthesize C-SGO.

3.3 Characteristics of materials

The synthesized C-SGO is functionalized with − SO_3H, − COOH, and − OH groups, which directly contribute to the catalysis efficiency [37]. In particular, − SO_3H and − COOH groups function as Brønsted acids during the furfural synthesis process, while − OH and − COOH groups could provide the hydrophilicity needed for the catalytic process [8].

SEM images, as shown in Fig. 4a–b, were used to determine the structure and morphology of C-GO8 and C-SGO. Regions of folds and folded plates are observed in both C-GO8 and C-SGO samples. Figure 4a shows that the C-GO8 structure resembles stacked sheets with various small flakes after sulfonation; SEM of C-SGO shows the structure is more wrinkled probably due to sulfonation. Comparing the respective SEM images of C-GO8 and C-SGO, the flakes seem nearly effectively removed from C-SGO. There is much similarity in the surface structures

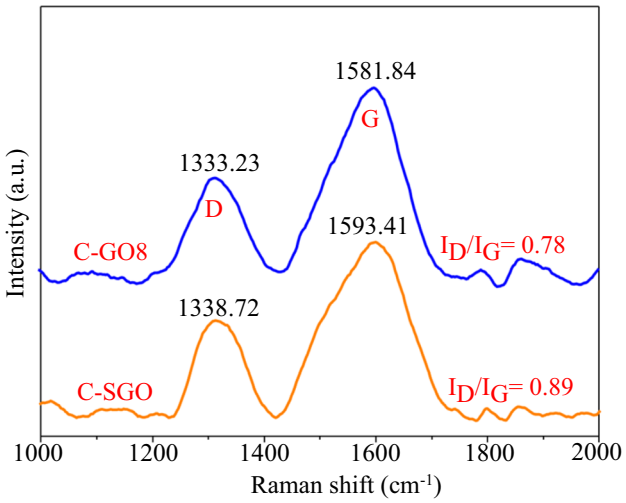

Fig. 5 Raman spectra of C-GO8 and C-SGO

of C-GO8 and C-SGO with previously reported syntheses from biomass [13].

Raman spectroscopy was used to further characterize the structure of C-GO8 and C-SGO, as shown in Fig. 5. The D band, which is related to defects in the carbon structure, is located at 1333.23 and 1338.72 cm^{-1} for C-GO8 and C-SGO samples, respectively. In turn, the G band exhibited at 1581.84 and 1593.41 cm^{-1} for C-GO8 and C-SGO represents oscillations of sp^2 bonded carbons in the graphite carbon layers. The I_D/I_G ratio is used as a measurement of defect sites in carbon materials — the lower the I_D/I_G ratio, the lower the proportion of disordered structures [11]. The change in I_D/I_G ratio from 0.78 to 0.89 indicates that, in comparison with C-GO8, sulfonation has led to an increase in the sp^3 carbon atom content of C-SGO [38].

Figure 6 illustrates the XRD pattern of C-GO8; the diffraction peak at 11.64°, corresponding to the (001) crystal plane with an interlayer distance (d) of 0.76 nm, is expected of the GO sheets. A wider reflection peak is also observed at 20.28°, with an interlayer distance of about 0.44 nm corresponding to reduced graphene oxide. Sulfonation of C-GO8

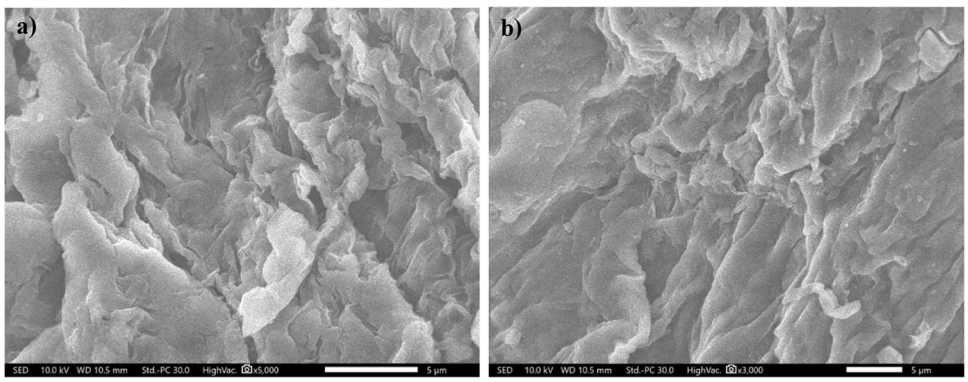

Fig. 4 SEM images of **a** C-GO8 and **b** C-SGO

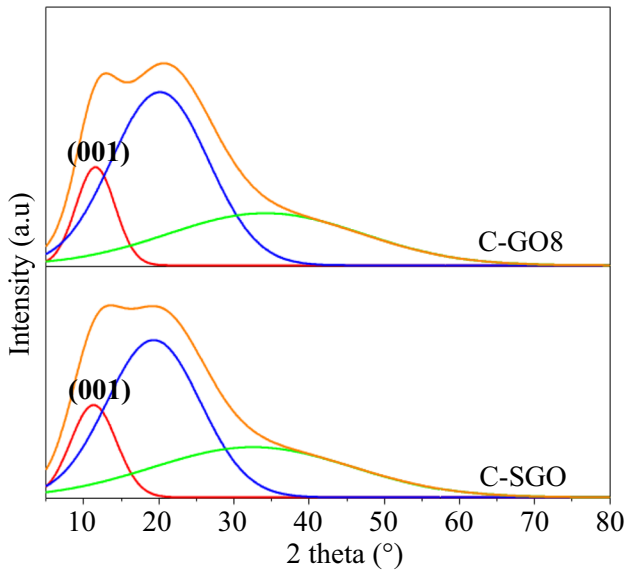

Fig. 6 XRD patterns of C-GO8 and C-SGO

reduces the interlayer distance to about 0.78 (nm). The XRD pattern of C-SGO is similar to that of C-GO8, showing that the addition of the $-SO_3H$ group does not greatly affect the structure of C-GO8 as shown in Fig. 6. The XRD pattern of the material samples exhibiting high background strength shows that C-GO8 and C-SGO contain a high proportion of disturbed materials in the form of amorphous carbon [39, 40].

The FTIR spectra of samples C-GO8 and C-SGO are shown in Fig. 7a. From the spectra, the presence of the carboxyl functional group and unconjugated ketone stretching (C = C) is indicated at 1620.62 and 1615.16 cm^{-1} for C-GO8 and C-SGO, respectively. The FTIR spectrum of C-SGO demonstrates a strong increase in the absorption intensity of the CO group at 1716 cm^{-1} compared with the CO group of C-GO8 at 1710.99 cm^{-1}. Furthermore, the peaks at 1156.85 and 1043.76 cm^{-1} of C-GO and 1060.60 and 1226.62 cm^{-1} of C-SGO are considered symmetric and asymmetric stretching oscillations of O = S = O, confirming the existence of the $-SO_3H$ group assigned as the Brønsted acid site [21, 41]. The presence of Fe − O bonding observed at 585 cm^{-1} in the spectrum of C-GO8 is attributed to the incomplete washing of ferrocene during the synthesis of the material. In the spectrum of C-SGO, however, the absorption peak for Fe − O was no longer recorded, revealing that the sulfonation process dissolved the remaining Fe [42].

Figure 7b shows the elemental distributions of C-GO8 and C-SGO. The composition of C and O elements accounts for the majority of the cellulose-based materials; meanwhile, the presence of Fe impurities can be explained by the incomplete washing of ferrocene from the sample. The elemental composition of the C-GO8 sample includes S accounting for 68.89 ± 0.13%, O accounting for 30.68 ± 0.20%, and Fe accounting for 0.43 ± 0.17%. Compared with C-GO8, the C content (67.48 ± 0.11%) in the sample C-SGO increased by 1.02%, and O content (32.37 ± 0.17%) increased by about 1.5%. The increase in oxygen content can be attributed mostly to the $-SO_3H$ groups attached to the material following sulfonation. On the other hand, additionally, Fe was confirmed to be absent in the sample C-SGO; this is likely explained by sulfuric acid dissolving iron into the solution during ultrasonication. The difference in percentage compositions of the elements, especially that of Fe, O, and S, has proved the successful attachment of $-SO_3H$ groups to the C-SGO material [16]. For the C-SGO sample after 5 reuse cycles, the contents of C and O were 65.46 ± 0.11% and 34.41 ± 0.17%, respectively, and the content of S (0.13 ± 0.02%) was slightly reduced compared to the original C-SGO sample. The observed results are the consequence of S leaching from the sample after multiple recoveries and reuse cycles, which may be considered as a cause of decreased furfural production efficiency [43].

Table 4 shows the BET surface area of C-SGO compared to other studies. The result shows that the specific surface

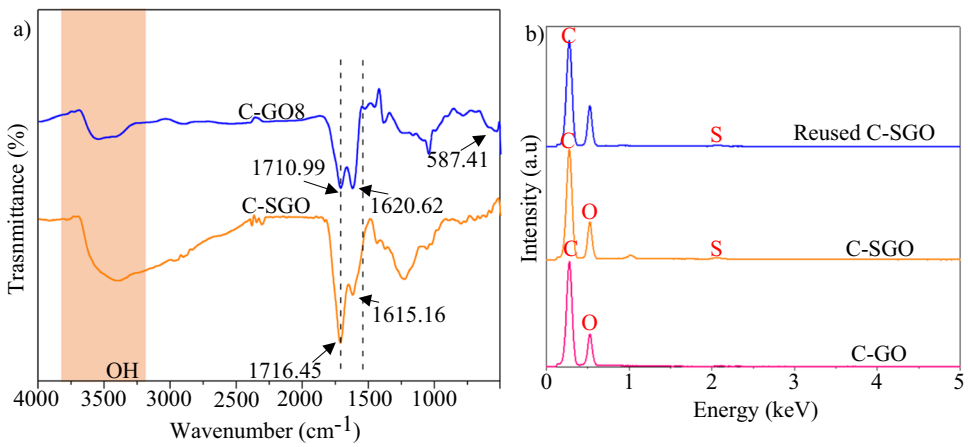

Fig. 7 **a** FTIR spectra and **b** EDS spectra of C-GO8 and C-SGO

Table 4 Physicochemical properties of sulfonated carbon catalysts

No	Catalysts	S_{BET} ($m^2.g^{-1}$)	V_{micro} ($cm^3.g^{-1}$)	Pore diameter (nm)	Ref
1	C-SGO	26.665	0.026	2.94	This study
2	SGO	77	0.010		[46]
3	SO_4^{2-}/SnO_2-CS	37.3	0.06	5.3	[47]
4	SC-FAR-800	32.56	0.018	3.25	[44]
5	FAS-4	113	0.16	5.57	[3]
6	SO_4^{2-}/SnO_2-Al_2O_3-CFA	27.141	0.021	3.093	[4]

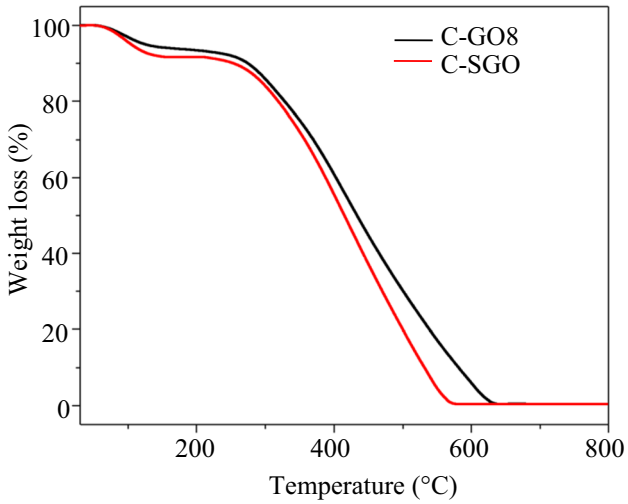

Fig. 8 TGA curves of C-GO8 and C-SGO

area of C-SGO is 26.665 $m^2.g^{-1}$, which is likely affected by the collapse of macropores during the sulfonation process. Additionally, the mounting of sulfonic groups on the surface of the material can contribute to a decrease in the specific surface area of the material [44]. The pore diameter is a key element of the catalyst in the reaction process; in C-SGO, pore diameters are distributed around 2.9 nm. Since this is larger than the molecular kinetic radius of xylose (0.86 nm) and furfural (0.68 nm), the reaction rate is enhanced by the ease of access for xylose to the catalytic site and the diffusion of furfural during the reaction [45].

As shown in Fig. 8, the TGA curve was performed over a temperature range of 0 to 800 °C in a nitrogen atmosphere to investigate the thermal stability of C-GO8 and C-SGO. A significant mass loss is detected from both samples. According to the diagram, we see that C-GO8 decomposes in three steps. The first mass loss (6%) takes place in the range of 50–150 °C due to the removal of water molecules. The decomposition of oxygen-containing functional groups takes place in the temperature range from 200 to 350 °C (19%). The gradient mass change observed at 400 °C indicates that there are amorphous carbons in the structure forming CO and escaping CO. The TGA curve of C-SGO is similar to that of C-GO8, but the mass loss in the second step is smaller, due to the lesser amount of oxygen-containing functional groups in that of C-GO8. C-GO8 and C-SGO materials are thermally stable at 650 and 570 °C, respectively [48, 49].

3.4 Effect of NaCl concentration on furfural yield

The hydrophilic functional groups (− OH and − COOH) in C-SGO enhanced the adsorption of xylose on the surface, and the functional group (− SO_3H) was assigned as the Brønsted acid site. The simultaneous presence of − SO_3H and hydrophilic functional groups in C-SGO increases the hydrolysis and dehydration capacity of xylan. Besides, the − SO_3H group generates a hydroxyl group on xylose to form furfural through dehydration to give a cyclic compound. Therefore, C-SGO is used to investigate the effect of NaCl concentration on furfural yield.

Figure 9 shows the influence of the dose of NaCl on the conversion of hemicellulose to furfural. As shown in Fig. 9, the conversion reaction was first carried out with a control containing only NaCl to demonstrate the role of the C-SGO as a catalyst. A furfural yield of 26.25% was achieved without the utilization of C-SGO. Simultaneously, the conversion of hemicellulose to furfural with C-SGO in presence of NaCl increases from 30.20 to 40.03%. The control result can be explained by the ability of Cl^- to break hydrogen bonds in biomass and form new hydrogen bonds with the − OH group in the hemicellulose–lignin matrix [47]. In addition, following the mechanism shown in Scheme 1, the Cl^- ion is capable of accelerating the formation of 1,2-enediol from the open-chain form of xylose [50]. However, at high NaCl concentrations, it is possible that excessive xylose formation instead promotes xylose dehydration and xylose–furfural polymerization, resulting in the formation of humins [5]. Therefore, the combination of 0.2 mol/L NaCl content with 10 wt% SGO catalyst gives the desired furfural yield of 40.03%.

The proposed route of the conversion of xylose into furfural is shown in Scheme 1. In the presence of heterogeneous catalysts, two processes occur: (1) the − SO_3H group breaks β-1,4 glycosidic bonds to produce monosaccharide (xylose);

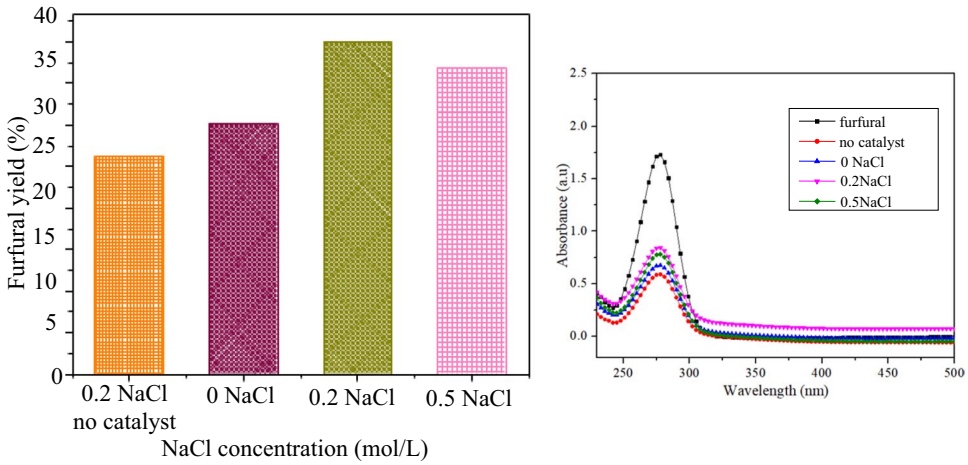

Fig. 9 Effect of NaCl concentration on furfural yield

(2) xylose will be isomerized to xylulose, which then forms xylofuranose and subsequently is dehydrated to create furfural or xylose will be dehydrated directly to furfural [2]. In the aldehyde group, electronegative oxygen promotes the formation of cationic carbon. As Cl^- attacks the C^+ of the intermediate, a reduction reaction occurs, and a π bond is formed between C_1 and C_2. This may explain the synergistic effect of NaCl in the acid-catalyzed dehydration of xylofuranose. The chloride ions interact with the hydroxyl groups via hydrogen bonding to form the unstable 1,2-enediol form, facilitating the formation of intermediates, and thereby promoting xylose conversion [50].

3.5 Reusability of the C-GO catalyst

The reusability of the material was investigated through 5 cycles under fixed reaction conditions of: reaction temperature 190 °C, reaction time 90 min, and catalyst amount 0.1 g. The C-SGO material was separated and washed with distilled water and ethanol after each reaction cycle. As shown in Fig. 10, the furfural efficiency gradually declined from 30.20 to 26.16% after 3 cycles and then dropped to 18.41 and 16.98% by cycles 4 and 5, respectively. This can be explained due to the loss of $-SO_3H$ functional groups on the C-SGO surface through the reduction of the S content of the reused C-SGO material, as demonstrated in Fig. 7b [51]. In addition, some impurities formed from side reactions deposited on the surface of the material reduce the catalytic sites, thereby reducing furfural efficiency [2].

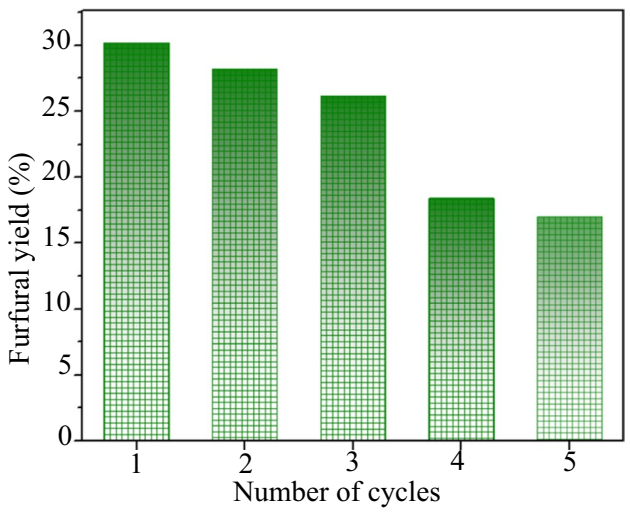

Fig. 10 Reusability of the C-SGO catalyst

The results of this research have demonstrated the usage of corncob biomass as a precursor for synthesizing catalysts with noteworthy furfural conversion performance and, in particular, highlighted the synergy of Lewis acid and Brønsted acid sites on the material. Similar studies have also shown that the usage of $FeCl_3$, $AlCl_3$, and NaCl as candidates for the Lewis acid sites provided good catalytic activity Similar studies have also shown that the usage of $FeCl_3$, $AlCl_3$, and NaCl as candidates for the Lewis acid sites provided good catalytic activity, due to the salts being able to form hydrolyzed metal species and H_3O^+ [4, 16]. The synthesis orientation of the material attaches metal salt to the carbon network to create coexisted Lewis acid and Brønsted acid sites, increasing the furfural yield. Overall, the synthesized C-SGO material shows promise for the development of future catalysts in furfural conversion applications.

4 Conclusion

In this study, the carbon-based acid catalyst material with a structure similar to graphene oxide (C-SGO) was successfully synthesized from corncob as a source of cellulose precursor, with $-SO_3H$ groups performing as the Brønsted acid catalytic site for application in furfural synthesis. SEM images showed that cellulose:ferrocene catalytic ratio of 1:1, with calcination at 300 °C for 30 min, results in a material with a corrugated structure. Synthesized

materials were sulfonated with sulfuric acid reagent at a concentration of 1 M for a desirable catalytic efficiency of 30.2%. In addition, synergistic catalytic effects were identified between C-SGO and NaCl; a furfural yield of 40.02% was obtained with 100 mg of C-SGO and 1 g hemicellulose introduced into a 200 °C reaction system for 90 min. Consequently, the study shows the potential of using seawater or wastewater containing NaCl as a low-cost reaction solvent in the process of converting hemicellulose to furfural. The C-SGO catalyst also shows good reusability after five recycles. Moreover, the utilization of cellulose from corncob in the synthesis of catalytic materials is regarded as an environmentally sustainable approach.

Acknowledgements We acknowledge the support of time and facilities from Ho Chi Minh City University of Technology (HCMUT), VNU-HCM for this study.

Author contribution Nguyen Minh Dat, Ninh Thi Tinh, Do Gia Nghiem, and Do Khanh Dan, experimental, data curation, and formal analysis; Ninh Thi Tinh, Huynh Thi Tuong Vy, Do Gia Nghiem, Nguyen Thi Phuong, and Tat Minh Hoang, writing—original draft preparation; Ninh Thi Tinh, Do Gia Nghiem, Pham Tan Khang, Le Minh Huong, and Nguyen Minh Dat, writing—review and editing; Mai Thanh Phong and Nguyen Huu Hieu, conceptualization and methodology and supervision. All authors have read and agreed to the published version of the manuscript.

Funding This research is funded by Ho Chi Minh City University of Technology — VNU-HCM, under grant number SVKSTN-2021-KTHH-18.

Data availability Not applicable.

Declarations

Conflict of interest The authors declare no competing interests.

References

1. Xu H, Xiong S, Zhao Y et al (2021) Conversion of xylose to furfural catalyzed by carbon-based solid acid prepared from pectin. Energy Fuels 35:9961–9969. https://doi.org/10.1021/acs.energyfuels.1c00628
2. Zhou N, Zhang C, Cao Y et al (2021) Conversion of xylose into furfural over MC-SnOx and NaCl catalysts in a biphasic system. J Clean Prod 311:127780. https://doi.org/10.1016/j.jclepro.2021.127780
3. Chatterjee A, Hu X, Lam FL-Y (2019) Modified coal fly ash waste as an efficient heterogeneous catalyst for dehydration of xylose to furfural in biphasic medium. Fuel 239:726–736. https://doi.org/10.1016/j.fuel.2018.10.138
4. Gong L, Xu Z-Y, Dong J-J et al (2019) Composite coal fly ash solid acid catalyst in synergy with chloride for biphasic preparation of furfural from corn stover hydrolysate. Bioresour Technol 293:122065. https://doi.org/10.1016/j.biortech.2019.122065
5. Teng X, Si Z, Li S et al (2020) Tin-loaded sulfonated rape pollen for efficient catalytic production of furfural from corn stover. Ind Crops Prod 151:112481. https://doi.org/10.1016/j.indcrop.2020.112481
6. Yang T, Li W, Ogunbiyi AT, An S (2021) Efficient catalytic conversion of corn stover to furfural and 5-hydromethylfurfural using glucosamine hydrochloride derived carbon solid acid in Y-valerolactone. Ind Crops Prod 161:113173
7. Zhu Y, Li W, Lu Y et al (2017) Production of furfural from xylose and corn stover catalyzed by a novel porous carbon solid acid in γ-valerolactone. RSC Adv 7:29916–29924. https://doi.org/10.1039/c7ra03995f
8. Dulie NW, Woldeyes B, Demsash HD (2021) Synthesis of lignin-carbohydrate complex-based catalyst from Eragrostis tef straw and its catalytic performance in xylose dehydration to furfural. Int J Biol Macromol 171:10–16. https://doi.org/10.1016/j.ijbiomac.2020.12.213
9. Ma J, Li W, Guan S et al (2019) Efficient catalytic conversion of corn stalk and xylose into furfural over sulfonated graphene in γ-valerolactone. RSC Adv 9:10569–10577. https://doi.org/10.1039/c9ra01411j
10. Dat NM, Thinh DB, Huong LM et al (2022) Facile synthesis and antibacterial activity of silver nanoparticles-modified graphene oxide hybrid material: the assessment, utilization, and anti-virus potentiality. Mater Today Chem 23:100738. https://doi.org/10.1016/j.mtchem.2021.100738
11. Sujiono EH, Zurnansyah ZD et al (2020) Graphene oxide based coconut shell waste: synthesis by modified Hummers method and characterization. Heliyon 6:e04568. https://doi.org/10.1016/j.heliyon.2020.e04568
12. Marcano DC, Kosynkin DV, Berlin JM et al (2010) Improved synthesis of graphene oxide. ACS Nano 4:4806–4814. https://doi.org/10.1021/nn1006368
13. Hashmi A, Singh AK, Jain B, Singh A (2020) Muffle atmosphere promoted fabrication of graphene oxide nanoparticle by agricultural waste. Fullerenes Nanotub Carbon Nanostructures 28:627–636. https://doi.org/10.1080/1536383X.2020.1728744
14. Tondro H, Zilouei H, Zargoosh K, Bazarganipour M (2021) Nettle leaves-based sulfonated graphene oxide for efficient hydrolysis of microcrystalline cellulose. Fuel 284:118975. https://doi.org/10.1016/j.fuel.2020.118975
15. Yan Y, Manickam S, Lester E et al (2021) Synthesis of graphene oxide and graphene quantum dots from Miscanthus via ultrasound-assisted mechano-chemical cracking method. Ultrason Sonochem 73:105519. https://doi.org/10.1016/j.ultsonch.2021.105519
16. Sun K, Shao Y, Liu P et al (2021) A solid iron salt catalyst for selective conversion of biomass-derived C5 sugars to furfural. Fuel 300:120990
17. Cai D, Chen H, Zhang C et al (2021) Carbonized core-shell diatomite for efficient catalytic furfural production from corn cob. J Clean Prod 283:125410
18. Zhao Y, Lu K, Xu H et al (2021) A critical review of recent advances in the production of furfural and 5-hydroxymethylfurfural from lignocellulosic biomass through homogeneous catalytic hydrothermal conversion. Renew Sustain Energy Rev 139:110706. https://doi.org/10.1016/j.rser.2021.110706
19. Huong LM, Trung TQ, Tuan TT et al (2022) Surface functionalization of graphene oxide by sulfonation method to catalyze the synthesis of furfural from sugarcane bagasse. Biomass Convers Biorefinery. https://doi.org/10.1007/s13399-021-02272-5
20. Kim JJ, Kwon YK, Kim JH et al (2014) Effective microwell plate-based screening method for microbes producing cellulase and xylanase and its application. J Microbiol Biotechnol 24:1559–1565. https://doi.org/10.4014/jmb.1405.05052
21. Ayyaru S, Ahn YH (2017) Application of sulfonic acid group functionalized graphene oxide to improve hydrophilicity, permeability, and antifouling of PVDF nanocomposite ultrafiltration membranes. J Memb Sci 525:210–219. https://doi.org/10.1016/j.memsci.2016.10.048

22. Qi Z, Wang Q, Liang C et al (2020) Highly efficient conversion of xylose to furfural in a water-MIBK system catalyzed by magnetic carbon-based solid acid. Ind Eng Chem Res 59:17046–17056. https://doi.org/10.1021/acs.iecr.9b06349
23. Chaturvedi V, Verma P (2013) An overview of key pretreatment processes employed for bioconversion of lignocellulosic biomass into biofuels and value added products. 3 Biotech 3:415–431. https://doi.org/10.1007/s13205-013-0167-8
24. Samanta AK, Senani S, Kolte AP et al (2012) Production and in vitro evaluation of xylooligosaccharides generated from corn cobs. Food Bioprod Process 90:466–474. https://doi.org/10.1016/j.fbp.2011.11.001
25. Ma L, Du L, Cui Y et al (2016) Isolation and structural analysis of hemicellulose from corncobs after a delignification pretreatment. Anal Methods 8:7500–7506. https://doi.org/10.1039/c6ay01863g
26. Zhang M, Wang F, Su R et al (2010) Ethanol production from high dry matter corncob using fed-batch simultaneous saccharification and fermentation after combined pretreatment. Bioresour Technol 101:4959–4964. https://doi.org/10.1016/j.biortech.2009.11.010
27. Araújo D, Castro MCR, Figueiredo A et al (2020) Green synthesis of cellulose acetate from corncob: physicochemical properties and assessment of environmental impacts. J Clean Prod 260:120865. https://doi.org/10.1016/j.jclepro.2020.120865
28. Araújo D, Vilarinho M, Machado A (2019) Effect of combined dilute-alkaline and green pretreatments on corncob fractionation: pretreated biomass characterization and regenerated cellulose film production. Ind Crops Prod 141:111785. https://doi.org/10.1016/j.indcrop.2019.111785
29. Reddy KO, Maheswari CU, Shukla M (2013) Physico-chemical characterization of cellulose extracted from ficus leaves. J Biobased Mater Bioenergy 7:496–499. https://doi.org/10.1166/jbmb.2013.1342
30. Banerjee S, Patti AF, Ranganathan V, Arora A (2019) Hemicellulose based biorefinery from pineapple peel waste: xylan extraction and its conversion into xylooligosaccharides. Food Bioprod Process 117:38–50. https://doi.org/10.1016/j.fbp.2019.06.012
31. Buslov DK, Kaputski FN, Sushko NI et al (2009) Infrared spectroscopic analysis of the structure of xylans. J Appl Spectrosc 76:801–805. https://doi.org/10.1007/s10812-010-9282-z
32. Giudicianni P, Cardone G, Ragucci R (2013) Cellulose, hemicellulose and lignin slow steam pyrolysis: thermal decomposition of biomass components mixtures. J Anal Appl Pyrolysis 100:213–222. https://doi.org/10.1016/j.jaap.2012.12.026
33 Yu H, Wang J, Yu JX et al (2020) Adsorption performance and stability of the modified straws and their extracts of cellulose, lignin, and hemicellulose for Pb2+: pH effect. Arab J Chem 13:9019–9033. https://doi.org/10.1016/j.arabjc.2020.10.024
34. Squinca P, Bilatto S, Badino AC, Farinas CS (2020) Nanocellulose production in future biorefineries: an integrated approach using tailor-made enzymes. ACS Sustain Chem Eng 8:2277–2286. https://doi.org/10.1021/acssuschemeng.9b06790
35. Teimuri-Mofrad R, Abbasi H, Hadi R (2019) Graphene oxide-grafted ferrocene moiety via ring opening polymerization (ROP) as a supercapacitor electrode material. Polymer (Guildf) 167:138–145. https://doi.org/10.1016/j.polymer.2019.01.084
36. Ashwin Karthick N, Thangappan R, Arivanandhan M et al (2018) A facile synthesis of ferrocene functionalized graphene oxide nanocomposite for electrochemical sensing of lead. J Inorg Organomet Polym Mater 28:1021–1028. https://doi.org/10.1007/s10904-017-0744-0
37. Lin Q, Zhang C, Wang X et al (2019) Impact of activation on properties of carbon-based solid acid catalysts for the hydrothermal conversion of xylose and hemicelluloses. Catal Today 319:31–40. https://doi.org/10.1016/j.cattod.2018.03.070
38. Yeleuov M, Daulbayev C, Taurbekov A et al (2021) Synthesis of graphene-like porous carbon from biomass for electrochemical energy storage applications. Diam Relat Mater 119:108560. https://doi.org/10.1016/j.diamond.2021.108560
39. Jeong H-K, Lee YP, Jin MH et al (2009) Thermal stability of graphite oxide. Chem Phys Lett 470:255–258. https://doi.org/10.1016/j.cplett.2009.01.050
40. Stobinski L, Lesiak B, Malolepszy A et al (2014) Graphene oxide and reduced graphene oxide studied by the XRD, TEM and electron spectroscopy methods. J Electron Spectros Relat Phenomena 195:145–154. https://doi.org/10.1016/j.elspec.2014.07.003
41. Dai Y, Yang S, Wang T et al (2022) High conversion of xylose to furfural over corncob residue-based solid acid catalyst in water-methyl isobutyl ketone. Ind Crops Prod 180:114781. https://doi.org/10.1016/j.indcrop.2022.114781
42. Nguyen H, … KD-S and, 2015 undefined synthesis of Fe3O4/graphene oxide nanocomposite for the treatment of heavy metals in the contaminated wastewater. stdj.scienceandtechnology.com.vn 18:
43. Wang X, Qiu M, Tang Y et al (2021) Synthesis of sulfonated lignin-derived ordered mesoporous carbon for catalytic production of furfural from xylose. Int J Biol Macromol 187:232–239. https://doi.org/10.1016/j.ijbiomac.2021.07.155
44. Huang T, Zhou Y, Zhang X et al (2022) Conversion of carbohydrates into furfural and 5-hydroxymethylfurfural using furfuryl alcohol resin-based solid acid as catalyst. Cellulose 29:1419–1433. https://doi.org/10.1007/s10570-021-04375-8
45. Gong L, Zha J, Pan L et al (2022) Highly efficient conversion of sunflower stalk-hydrolysate to furfural by sunflower stalk residue-derived carbonaceous solid acid in deep eutectic solvent/organic solvent system. Bioresour Technol 351:126945. https://doi.org/10.1016/j.biortech.2022.126945
46. Ogino I, Suzuki Y, Mukai SR (2018) Esterification of levulinic acid with ethanol catalyzed by sulfonated carbon catalysts: promotional effects of additional functional groups. Catal Today 314:62–69. https://doi.org/10.1016/j.cattod.2017.10.001
47. Ji L, Tang Z, Yang D et al (2021) Improved one-pot synthesis of furfural from corn stalk with heterogeneous catalysis using corn stalk as biobased carrier in deep eutectic solvent–water system. Bioresour Technol 340:125691. https://doi.org/10.1016/j.biortech.2021.125691
48. Chakraborty V, Das P, Roy PK (2021) Graphene oxide–coated pyrolysed biochar from waste sawdust and its application for treatment of cadmium-containing solution: batch, fixed-bed column, regeneration, and mathematical modelling. Biomass Convers Biorefinery. https://doi.org/10.1007/s13399-020-01153-7
49. Loryuenyong V, Totepvimarn K, Eimburanapravat P, et al (2013) Preparation and characterization of reduced graphene oxide sheets via water-based exfoliation and reduction methods. Adv Mater Sci Eng 2013:
50. Li Z, Luo Y, Jiang Z et al (2020) The promotion effect of NaCl on the conversion of xylose to furfural†. Chinese J Chem 38:178–184. https://doi.org/10.1002/cjoc.201900433
51. Jia Q, Teng X, Yu S et al (2019) Production of furfural from xylose and hemicelluloses using tin-loaded sulfonated diatomite as solid acid catalyst in biphasic system. Bioresour Technol Reports 6:145–151. https://doi.org/10.1016/j.biteb.2019.03.001